

The derivation of the cellulose microfibril angle by small-angle X-ray scattering from structurally characterized softwood cell-wall populations

Kenneth M. Entwistle,^{a*} Stephen J. Eichhorn^a and Namasivayam Navaranjan^b

^aMaterials Science Centre, School of Materials, University of Manchester, Grosvenor Street, Manchester M1 7HS, UK, and ^bEnsis Papro, Forestry Research, Roturua, New Zealand.
Correspondence e-mail: ken.entwistle@manchester.ac.uk

Received 13 January 2005
Accepted 15 March 2005

A method is presented for the measurement, using small-angle X-ray scattering (SAXS), of the microfibril angle and the associated standard deviation for the cellulose microfibrils in the S₂ layer of the cell walls of softwood specimens. The length and orientation of over 1000 cell walls in the irradiated volume of the specimen are measured using quantitative image analysis. From these data are calculated the azimuthal variation of the scattered intensity. The calculated values are compared with the measured values. The undetermined parameters in the analysis are the microfibril angle (M) and the standard deviation (σ_ϕ) of the intensity distribution arising from the wandering of the fibril orientation about the mean value. The two parameters are varied to give the best fit between the calculated and the measured values. Six separate pairs of values are determined for six different values of the angle of incidence of the X-ray beam relative to the normal to the radial direction in the specimen. The results show good agreement. The azimuthal distribution of scattered intensity for the real cell-wall structure is compared with that calculated for an assembly of rectangular cells with the same ratio of transverse to radial cell-wall lengths. Despite the existence of marked differences in the intensity distributions around the zero azimuth angle, the position of the extreme flanks of the distribution is very close for the real and the rectangular cells. This means that useful values of the microfibril angle can be obtained from the curve for the real cells using the Meylan parameter T derived by drawing tangents to the flanks of the intensity distribution and using $M = kT$. The value of k is $M/(M + 2\sigma_\phi)$. Since both of these parameters are determined in the work now described, k is also determined. It is also demonstrated that for $\beta = 45^\circ$ (where β is the angle between the plane face of the wood specimens and the radial direction) the peaks in the azimuthal intensity distribution for the real and the rectangular cells coincide. If this peak position is Φ_{45} , then the microfibril angle can be determined from the relation $M = \tan^{-1}(\tan \Phi_{45}/\cos 45^\circ)$, which is precise for rectangular cells.

© 2005 International Union of Crystallography
Printed in Great Britain – all rights reserved

1. Introduction

The orientation of the cellulose microfibrils in the S₂ layers of the cell walls of softwood has a significant influence on the elastic and the water-dependent properties. For this reason, considerable effort has been directed towards the measurement of the cellulose microfibril angle (M). Direct measurement of M has been made (Senft & Bendtsen, 1985) by highlighting the microfibrils in individual cell walls with iodine staining, but the most widely adopted techniques use either wide-angle X-ray diffraction or small-angle X-ray scattering. The pioneering work of Meylan (1967) and of Cave (1966) led to the use of the ' T ' parameter derived from the azimuthal distribution of the intensity diffracted by the (002) planes of

the monoclinic cellulose fibrils. Evans (1999) has demonstrated that the second moment of the same intensity distribution about the mean is simply related to M and this is used to determine M with the SilviScan equipment. Measurements of the microfibril angle using small-angle X-ray scattering on single wood fibres have been pioneered by Müller *et al.* (1998). Additionally, Reiterer *et al.* (1998) also mention the use of SAXS to investigate the spiral angle (or microfibril angle) in wood cell walls, but their primary assumption in the analysis is that the wood cell walls are square.

Reiterer *et al.* (1998) varied the angle of the X-ray beam to the specimen surface, but they assume in the interpretation of the scattering that all radial walls are parallel, and indeed the same for the transverse walls. We have previously explored the

extent to which it is necessary to take into account the detailed cell structure in order to interpret diffraction and scattering data (Entwistle & Navaranjan, 2002). This involved using quantitative image analysis to measure the length and the orientation of over 1000 cell walls in the irradiated volume of the specimen. From these data, the azimuthal angle of the peak scattering intensity Φ_p was calculated for a specimen irradiated in a direction at 45° to the radial and the transverse directions. It was thereby demonstrated that the microfibril angle could be derived from

$$M = \tan^{-1}(\tan \Phi_p / \cos 45^\circ), \quad (1)$$

with an error of about 1° . This relation is exact for rectangular cells.

In the present paper we describe a more detailed investigation based on the same approach. However, we report and emphasize results pertaining to the effect of orientation of *each* cell wall relative to the direction of the X-ray beam, which differs in the approach used by other authors (Reiterer *et al.*, 1998). The essence is the following. We first determine using quantitative image analysis the length and the orientation of about 1000 cell walls in the irradiated volume of the specimen. From these data the azimuthal distribution of small-angle scattered intensity is calculated. The two significant parameters in the analysis are the microfibril angle M and the standard deviation of the scattering σ_ϕ caused by the orientation spread of the constituent fibrils. These two parameters are initially undetermined. The small-angle scattered intensity is measured using a synchrotron source and the calculated intensity is adjusted to fit the measured intensity by varying M and σ_ϕ . This is very conveniently done using a spreadsheet. The values of M and σ_ϕ that give the best fit emerge as the measured values. Confidence in the values was enhanced by carrying out six experiments in which the X-ray beam was directed at different angles of incidence relative to the normal to the radial plane.

2. Experimental

Small-angle scattering specimens, $10 \times 2 \times 1$ mm, were cut from one early-wood growth ring in a block of *Pinus sylvestris*. Specimens of six different orientations were cut as indicated in Fig. 1. The angle β shown is between the wider face of the specimen and the radial direction. The specimens were all irradiated with the X-ray beam (0.6 mm in size) directed normal to the wider face; thus β is the angle between the normal to the radial plane and the direction of the X-ray beam. The various cell-wall orientations were obtained by cutting specimens as shown in Fig. 1 so that the scattered radiation would pass through the same length of specimen material in all cases.

Small-angle scattering intensity patterns were produced for the six specimens on beamline 2.1 at the Daresbury Synchrotron. The X-ray wavelength was 0.15 nm and the scattering pattern was recorded on an area detector 2.5 m from the specimen. A typical pattern is shown in Fig. 2. The

azimuthal variation of scattered intensity was measured by integrating radially over a narrow annulus at a radius of 100 pixels. A typical intensity distribution is shown in Fig. 3. The prominent pairs of peaks arise from the S_2 layers and the intermediate lower peaks are generated by the S_1 and S_3 microfibrils. The S_2 scattered intensity was determined by subtracting the background intensity from the measured

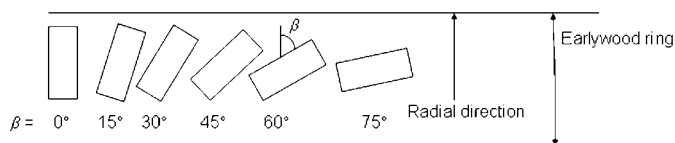


Figure 1
Diagram showing the orientation of the cross section of the SAXS specimens cut from a single early-wood ring. The vertical arrow is the radial direction and β is the angle between the radial direction and the irradiated face of the specimen.

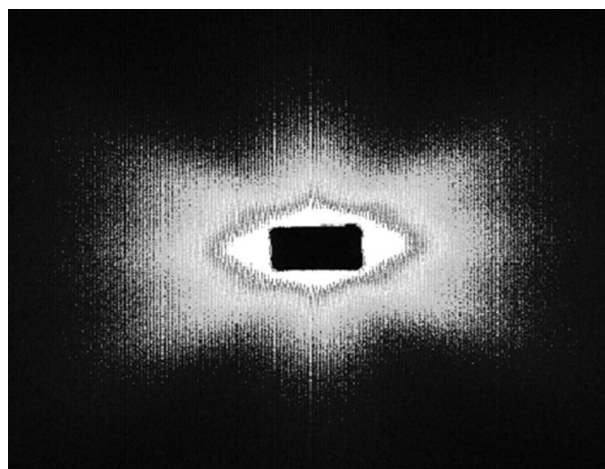


Figure 2
Small-angle scattering pattern for a specimen with the X-ray beam directed normal to the radial plane ($\beta = 0^\circ$).

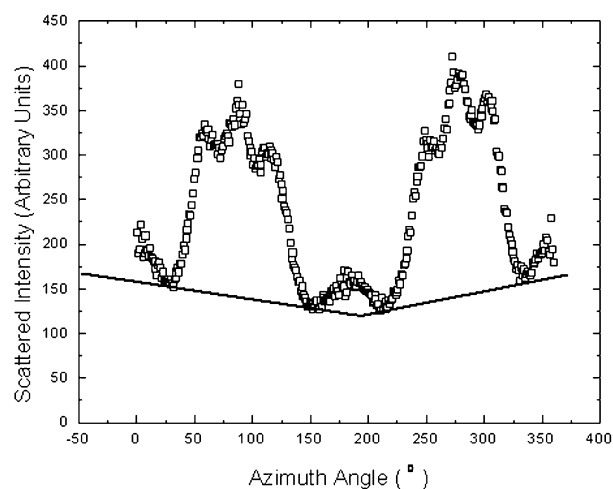


Figure 3
The azimuthal distribution of scattered X-ray intensity for a specimen irradiated in a direction normal to the radial plane ($\beta = 0^\circ$). The intensity was measured at a radius of 100 pixels from the origin. The detector was 2.5 m from the specimen. The black line is the subtracted background.

curve. This was judged to be the base line drawn tangentially to the minima indicated in Fig. 3. A second determination of the intensity distribution using an annulus at a radius of 140 pixels gave peak azimuth angles identical to those for the 100 pixels data. Azimuthal spreading, due to the convolution of the beam profile, is thought to be insignificant due to the fact that the intensity distribution for $R = 100$ and 140 was found to be the same. Since the azimuthal angular range of the spread gets less as R increases, we conclude that the effect of the beam geometry is negligible.

The length and the orientation of over 1000 cell walls were measured using a Scion Image Analyser. A section in the R-T (radial-transverse) plane was cut with a sharp knife blade. The coordinates of the cell-wall junctions were measured relative to orthogonal axes directed in the radial and the transverse directions. From these data, the length of each cell wall in the R-T plane and its orientation relative to the radial direction were determined. The total cell-wall length within a one degree range of orientation was collected. The 180 values are plotted in Fig. 4. The radial walls are those between 45° and -45° the remainder are the transverse walls. The total length of the radial walls is 1.82 times the length of the transverse walls. The distribution of the orientation of the radial walls is wider than that of the transverse walls and shows a hint of a bimodal pattern. We return later to this feature.

2.1. The calculation of the azimuthal variation of the scattered intensity

The equations used to calculate the scattered intensity were derived by Entwistle & Navaranjan (2002). We outline here the essential steps in the analysis.

In Fig. 5, z is the direction of the cell axis, y is the radial direction and x is the transverse direction. A cell wall is shown with two sets of S_2 microfibrils f_1 and f_2 lying at the microfibril angle M to the cell axis direction z . The incident X-ray beam is directed along the x axis. The normal to the cell wall lies at an

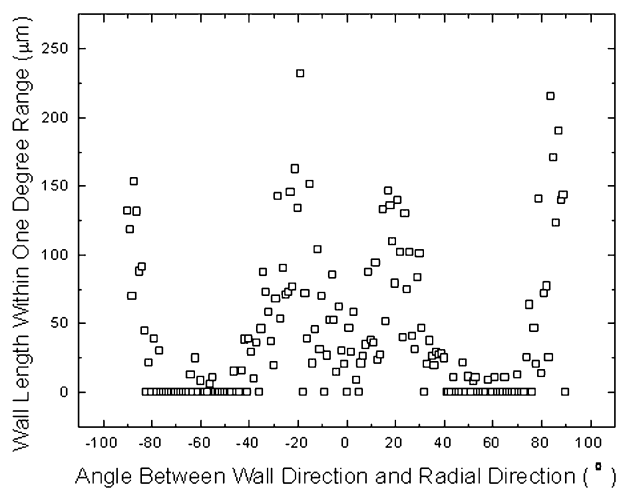


Figure 4
The total length of cell wall within a one degree range plotted against the mean orientation θ relative to the radial direction. Radial walls lie around $\theta = 0^\circ$ and transverse walls around $\pm 90^\circ$.

angle α to the direction of the X-ray beam. The azimuth angle Φ_1 for the scattered intensity from the fibrils f_1 is given by

$$\tan \Phi_1 = -\cos \alpha \tan M \quad (2)$$

and the corresponding azimuth angle Φ_2 for scattering from f_2 is given by

$$\tan \Phi_2 = -\cos(\alpha + \pi) \tan M = \cos \alpha \tan M, \quad (3)$$

and so $\Phi_1 = -\Phi_2$ and the scattered intensity is symmetrical about $\Phi = 0^\circ$.

A specimen is cut so that the radial direction is at an angle β to the front face of the specimen (Fig. 6) and the X-rays are directed normal to the front face. For a cell wall lying at an angle θ to the radial direction, the value of α (see Fig. 5) is

$$\alpha = (\beta + \theta), \quad (4)$$

and thus the azimuthal angle for scattering from the f_1 fibrils in the cell wall is given from equation (2) by

$$\tan \Phi_1 = -\cos(\beta + \theta) \tan M, \quad (5)$$

and for scattering from the f_2 microfibrils, Φ_2 is given from equation (3) by

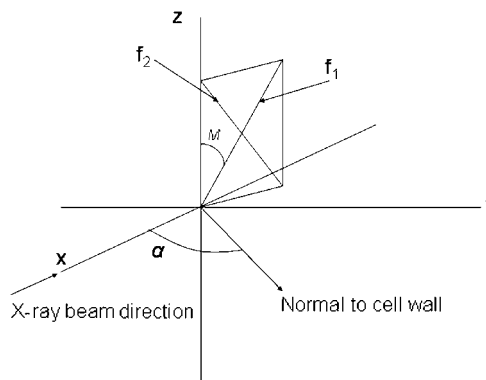


Figure 5
Diagram showing the relationship between a cell wall, the two S_2 microfibrils and the direction of the X-ray beam.

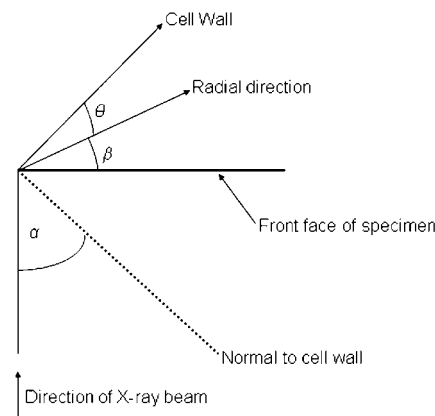


Figure 6
Diagram showing the relation between the front face of the specimen, the radial direction (β), the cell-wall direction (θ) and the direction of the X-ray beam normal to the face of the specimen.

$$\tan \Phi_2 = \cos(\beta + \theta) \tan M. \quad (6)$$

Measurements on six specimens will be reported later for which

$$\beta = 0, 15, 30, 45, 60 \text{ and } 75^\circ.$$

Round a circle located at the centre of the scattering pattern, the radiation intensity will be proportional to the strength of the scattering source. For an individual cell wall this will be proportional to its length. Further, the scattered intensity will be spread circumferentially round the circle because the orientation of the fibrils that make up the cellulose fibres wander to some degree around the average orientation. We assume that this distribution of scattered intensity can be represented by a Gaussian curve. So for a cell wall of length ΔL_n lying in a cell wall whose normal lies at an angle α_n to the ray beam, the azimuthal distribution of scattered intensity ΔI_{n1} is

$$\Delta I_{n1} = \Delta L_n \exp\left\{-\frac{1}{2}\left[\frac{(\Phi - \Phi_{n1})}{\sigma_\Phi}\right]^2\right\}, \quad (7)$$

where Φ_{n1} is the azimuthal angle for peak scattering given by equation (4) and σ_Φ is the standard deviation of the intensity distribution. The corresponding scattered intensity from the f_2 fibrils in the cell wall is given by

$$\Delta I_{n2} = \Delta L_n \exp\left\{-\frac{1}{2}\left[\frac{(\Phi - \Phi_{n2})}{\sigma_\Phi}\right]^2\right\}, \quad (8)$$

where Φ_{n2} is the azimuthal angle for peak scattering given by equation (5).

The azimuthal distribution of the total scattered intensity from the specimen is derived in the following way. For a particular cell-wall orientation θ , the total cell-wall length ΔL_n lying between $\pm 0.5^\circ$ of the value of θ is extracted from Fig. 4. The azimuthal variation of the scattered intensity from the f_1 microfibrils in that group of cell walls is

$$\Delta I_{n1} = \Delta L_n \exp\left\{-\frac{1}{2}\left[\frac{(\Phi - \Phi_{n1})}{\sigma_\Phi}\right]^2\right\} \quad (9)$$

and

$$\Phi_{n1} = \tan^{-1}[-\cos(\beta + \alpha) \tan M]. \quad (10)$$

This gives the intensity distribution as a function of Φ , the azimuth angle which ranges from -60 to 60° ; outside this range the scattered intensity is very small. The calculation is repeated for all of the 180 values of θ between -90° and 90° . The calculations are carried out using a Microsoft *Excel* spreadsheet in which the 121 columns are values of Φ and the rows are values of θ .

The scattering from the f_2 microfibrils is calculated on the basis that the f_2 fibrils can be considered to be f_1 fibrils in cell walls rotated through 180° . So the intensity can be calculated from equations (9) and (10) with values of θ lying between

$$\theta = -90^\circ + 180^\circ = 90^\circ \text{ and } \theta = 90^\circ + 180^\circ = 270^\circ.$$

The total spreadsheet comprises 360 rows, 180 for scattering from the f_1 microfibrils and 180 for scattering from the f_2 microfibrils. The azimuthal variation of scattered intensity is obtained by adding the intensity in each column, which gives

Table 1

Values of the microfibril angle M and the standard deviation σ_Φ that give the best fit between the measured and the calculated intensities.

β is the angle between the direction of the incident X-ray beam and the normal to the radial plane.

β ($^\circ$)	M ($^\circ$)	σ_Φ ($^\circ$)
0	31	10
15	34	9
30	37	8
45	35	10
60	36	9
75	36	8

the intensity for 121 values of Φ ranging from -60° to 60° . These values are plotted in the spreadsheet.

The two initially undetermined parameters are M and σ_Φ . These are determined by plotting the calculated and the measured intensity distributions, scaled to the same values, and adjusting M and σ_Φ to give the best fit. This can be done simply and elegantly on the spreadsheet. This procedure is carried out for six different angles of incidence of the X-rays relative to the radial plane on six spreadsheets.

3. Calculated and experimental results

Fig. 7 presents the measured small-angle scattering and the best fit calculated values for the six different incident radiation directions. Table 1 reports the best fit values for M and for σ_Φ . As can be seen, there is reasonable consistency between the values derived from the six specimens. It is clear that the lower values of β give lower values of M and that the outer flanks of the intensity distributions are critical features of the fit. For values of β less than 45° , these flanks are generated by the radial walls, and for angles greater than 45° , by the transverse walls. So the data of Table 1 indicate that possibly the value of M for the radial walls is slightly less than that for the transverse walls.

3.1. Comparison of the derived microfibril angle with that determined by other methods

3.1.1. The 'T' parameter. The microfibril angle can be deduced using the Meylan (1967) method from Fig. 7(a). The 'T' parameter was developed for wide-angle diffraction data but there is no reason in principle why it should not be used for small-angle scattering intensity distributions. Cave (1966) deduced that

$$T = M + 2\sigma. \quad (11)$$

The data in Table 1 suffice to derive T from this relation. Using the data for $\beta = 0^\circ$ in Table 1, one can say

$$T = 31 + 2(10) = 51^\circ.$$

Meylan (1967) uses the relation

$$M = kT. \quad (12)$$

Hence

$$k = 31/51 = 0.61. \quad (13)$$

This value is close to that put forward by Meylan (1967), which is here confirmed by an independent method. Not surprisingly, if T is determined by drawing tangents to the outer flanks of the curve in Fig. 6(a), a value of $M = 31^\circ$ results.

3.1.2. Azimuth angle for peak intensity for $\beta = 45^\circ$. The intensity distribution for $\beta = 45^\circ$ is plotted in Fig. 7(d). The

peak intensity is at $\Phi = 26.0^\circ$. The relation between this azimuth angle and M for rectangular cells is

$$M = \tan^{-1}(\tan \Phi_{45} / \cos 45^\circ), \quad (14)$$

giving $M = 34.6^\circ$. The measured value is 35° , so the use of the relation for rectangular cells to interpret the measured data gives a good estimate of M .

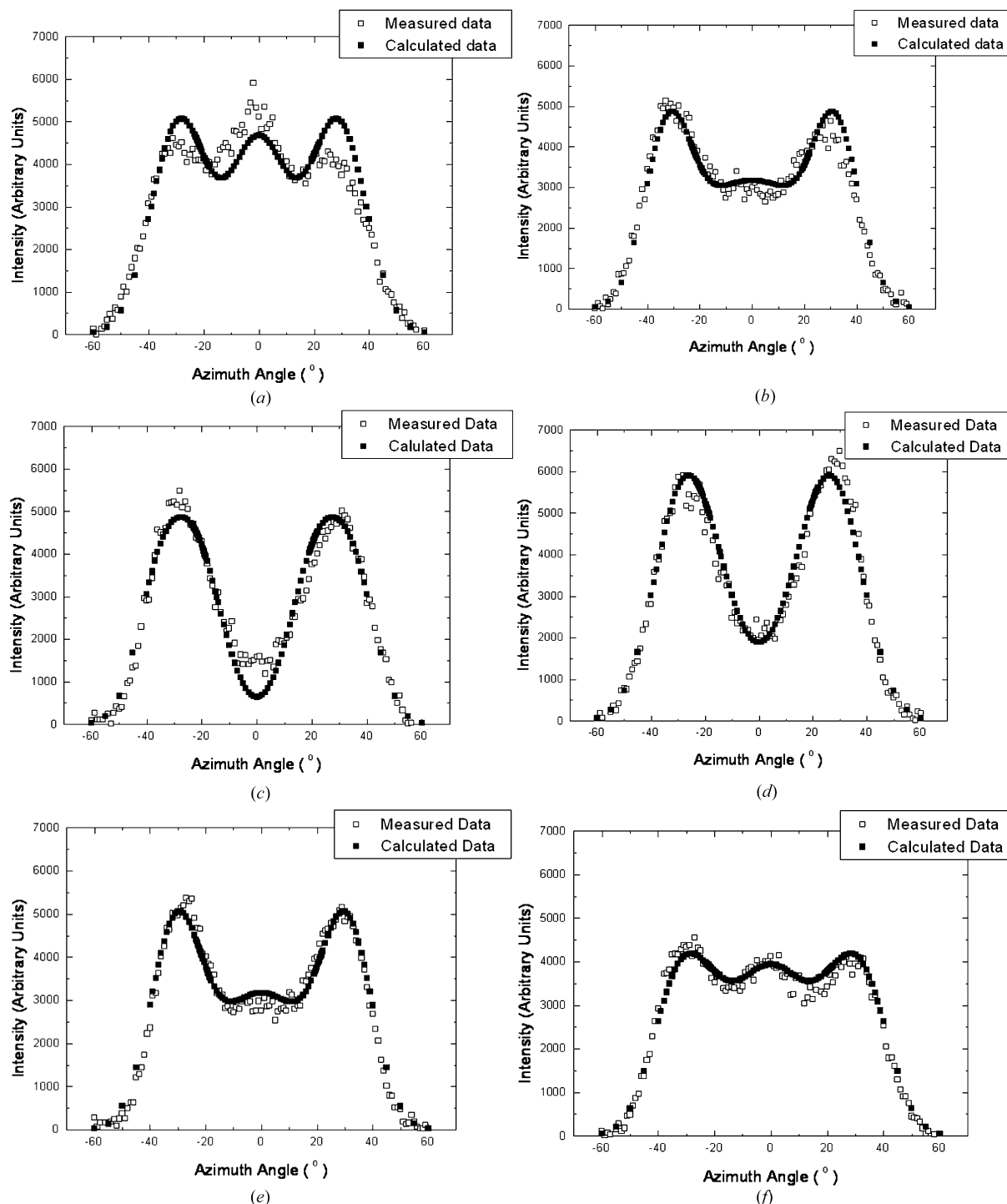


Figure 7 Comparisons between measured intensities (open squares) and calculated best fit intensities (solid squares) where (a) $\beta = 0^\circ$, best fit values $M = 31^\circ$ and $\sigma_\Phi = 10^\circ$; (b) $\beta = 15^\circ$, best fit values $M = 34^\circ$ and $\sigma_\Phi = 9^\circ$; (c) $\beta = 30^\circ$, best fit values $M = 37^\circ$ and $\sigma_\Phi = 8^\circ$; (d) $\beta = 45^\circ$, best fit values $M = 35^\circ$ and $\sigma_\Phi = 10^\circ$; (e) $\beta = 60^\circ$, best fit values $M = 36^\circ$ and $\sigma_\Phi = 9^\circ$; and (f) $\beta = 75^\circ$, best fit values $M = 36^\circ$ and $\sigma_\Phi = 9^\circ$.

3.2. Comparison of the distribution of scattered intensity from the real cell structure and from an assembly of rectangular cells

It is of interest to examine the nature and the extent of the differences between the intensity distributions scattered by the real cell structure and by an idealized structure of rectangular walls. We consider a rectangular structure in which the ratio of the total length of radial walls to the total length of transverse walls is the same as that for the real structure, which is 1.82. The intensity distributions for the real and the rectangular cells are compared in Fig. 8 for three cases in which the incident X-rays are at angles $\beta = 0, 45$ and 90° . The values assumed for M and σ_Φ are those that give the best fit to the measured data. There are no measured data for $\beta = 90^\circ$ so we use the data for $\beta = 75^\circ$.

Fig. 9 shows the variation of the azimuthal angle Φ for a single microfibril f (see Fig. 5) as the angle α between the normal to the cell wall in which the microfibril lies and the direction of the incident X-ray beam increases. The plotted curve is obtained from

$$\Phi = \tan^{-1}(\cos \alpha \tan 31^\circ), \quad (15)$$

where M , the microfibril angle, is 31 in this example. The significant point to note about Fig. 9 is that the azimuthal angle Φ is relatively insensitive to changes of α around $\alpha = 0^\circ$, that is for conditions where the X-ray beam is normal to the cell-wall plane, but is very sensitive to changes of α around $\alpha = 90^\circ$ where the beam lies in the plane of the wall.

We look first at Fig. 8(a) for which $\alpha = 0^\circ$. The curve for the rectangular cells shows two outer peaks from the f_1 and f_2 fibrils in the radial walls. The peaks are sharp because all the walls are parallel, so the profile is Gaussian with a standard deviation of σ_Φ . The X-rays are normally incident on these walls, so the peaks lie at $\Phi = M = 31$. The central peak arises from the f_1 and f_2 fibrils in the transverse wall. They both scatter at $\Phi = 0^\circ$ so their peaks superimpose. The intensity from the real cells shows a similar peak structure. The outer peaks again derive from the radial walls and are quite sharp. It is evident from Fig. 4 that the radial walls span a wide range of orientation. However, Fig. 9 shows that since the X-ray beam is normal to the radial plane ($\alpha = 0^\circ$), that range of orientation produces only a small change of azimuth angle. For example, a range of α from 0° to 25° corresponds to a range of Φ of only 1.5° . The peaks lie at $\pm 29.5^\circ$, which is only 1.5° from the values for rectangular cells. The peak at $\Phi = 0^\circ$ is from the transverse walls. It is evident from Fig. 4 that these cover a more compact spread of orientation than do the radial walls with a well defined maximum at $\theta = \pm 90^\circ$. This maximum generates a scattering peak at $\Phi = 0^\circ$. The peak is broader than that for the rectangular cells because of the spread resulting from the spread of transverse wall orientations.

A prominent feature of Fig. 8(a) is that the outer flanks of the curves for the real cells and the rectangular cells are close together. This means that if tangents are drawn to the outer flanks to determine the Meylan T value, both curves will give similar values for the microfibril angle.

As the angle of incidence of the X-ray beam β moves away from the radial plane, the outer peaks due to the radial walls move inwards and the central peak due to the transverse walls divides into two and both parts move symmetrically outwards.

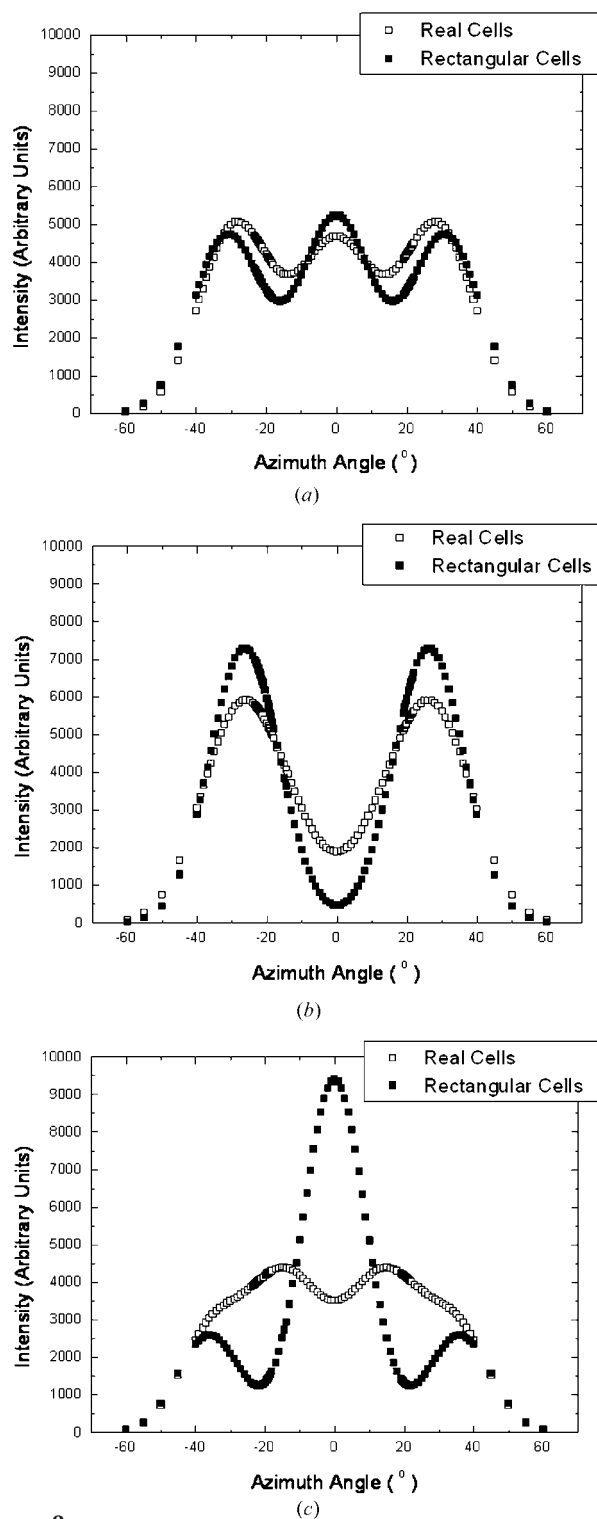


Figure 8 Comparisons between the scattering intensity from real wood cells (open squares) and rectangular cells (solid lines) with the same ratio of radial wall length to transverse wall length (1.82) for (a) $\beta = 0^\circ$, $M = 31^\circ$ and $\sigma_\Phi = 10^\circ$; (b) $\beta = 45^\circ$, $M = 35^\circ$ and $\sigma_\Phi = 10^\circ$; and (c) $\beta = 90^\circ$, $M = 36^\circ$ and $\sigma_\Phi = 9^\circ$.

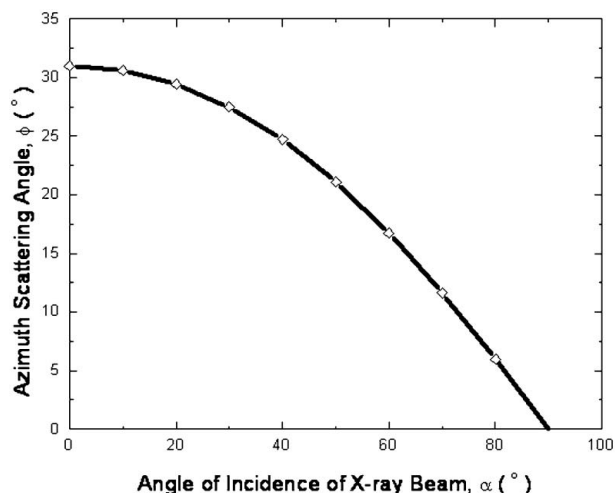


Figure 9
Variation of the azimuthal scattering angle Φ for a microfibril in a cell wall as the angle α between the normal to the cell wall and the direction of the X-ray beam increases (see Fig. 5). The fitted curve is the function $\Phi \tan^{-1}(\cos \alpha \tan 31^\circ)$.

When β reaches 90° , the outer peaks are from the transverse walls. The calculated intensity distributions for the real and for the rectangular cells are plotted in Fig. 8(c). They are markedly different. The curve for the rectangular cells shows two outer peaks due to the transverse walls with maxima at $\Phi = 36^\circ$, the microfibril angle. The central peak is due to the radial walls and its height is the result of the superposition of the f_1 and the f_2 scattering. The curve for the real cell structure is more complex. The curve shows two peaks at $\pm 14.7^\circ$ from the radial walls. The peaks occur because of the wide spread of orientation of the radial walls combined with a value of β near 90° produces, as Fig. 9 demonstrates, a wide range of azimuth angle. The outer flanks of the distribution are the sides of the lower peaks from the transverse walls that overlap those from the radial walls. It is remarkable that the outer flanks of the curves for the real cells and the rectangular cells coincide closely. So if tangents are drawn to the outer flanks to determine the microfibril angle by the Meylan T parameter, both curves would give a similar value. The value of T is 54.5° . If we determine the value of T from the known values of M and σ_Φ , then

$$T = M + 2\sigma_\Phi. \quad (16)$$

Thus

$$T = 36 + 2(9) = 54^\circ,$$

which is close to the measured value from both curves. So despite the dramatic difference between the two intensity distributions around $\Phi = 0^\circ$, the outer flanks are close together because the compact distribution of real transverse cell-wall

orientation produces scattering similar to that from the transverse walls of the rectangular cells.

In Fig. 8(b) for $\beta = 45^\circ$, the radial and transverse peaks have moved to converge. We have already seen that the value of the azimuth angle Φ_{45} at the peak can be used to obtain a value for the microfibril angle using

$$M = \tan^{-1}(\tan \Phi_{45} / \cos 45^\circ). \quad (17)$$

4. Conclusion

Values for the microfibril angle M and for the related standard deviation σ_Φ have been obtained for real wood cell structures using small-angle X-ray scattering. The azimuthal distribution of scattered intensity was calculated from the measured length and orientation of over 1000 cell walls. Values of M and σ_Φ , which are initially undetermined parameters in the analysis, were obtained by varying them to obtain the best fit between the calculated and the measured intensity distributions.

A comparison between the calculated intensity distributions for the real cell-wall structure and for an equivalent rectangular cell-wall structure revealed that significant differences were evident around $\Phi = 0^\circ$. However the extreme flanks of the distributions were close together and it is shown that useful values of M could be obtained by drawing tangents to the flanks of the measured curve and extracting the Meylan T value. The microfibril angle is then given by

$$M = 0.61T. \quad (18)$$

It was also found that the peaks of the intensity distributions for the real and the rectangular structures irradiated in a direction at 45° to the radial plane were close together. So the microfibril angle can be determined from the following relation, which is precise for rectangular cells:

$$M = \tan^{-1}(\tan \Phi_p / \cos 45^\circ). \quad (19)$$

The authors are grateful for experimental support from Gunter Grössman at the Daresbury Synchrotron and to the CCLRC for use of their facilities.

References

- Cave, I. D. (1966). *Forest Prod. J.* **16**, 37–42.
- Entwistle, K. M. & Navaranjan, N. (2002). *J. Mater. Sci.* **37**, 539–545.
- Evans, R. (1999). *Appita*, **52**, 283–290.
- Meylan, B. A. (1967). *Forest Prod. J.* **17**, 51–58.
- Müller, M., Czihak, C., Vogl, G., Fratzl, P., Schober H. & Riekkel, C. (1998). *Macromolecules*, **31**, 3953–3957.
- Reiterer, A., Jakob, H. F., Stanzl-Tscheegg, S. E. & Fratzl, P. (1998). *Wood Sci. Technol.* **32**, 335–345.
- Senft, J. F. & Bendtsen, B. A. (1985). *Wood Fibre Sci.* **17**, 564–567.